28

NACA-0012翼周りの遷音速流の計算

アンデイ・エカ・サキャ* 中村佳朗* 保原 充*

Transonic Flow Calculation around NACA-0012

by

Andi Eka SAKYA, Yoshiaki NAKAMURA and Michiru YASUHARA
Dept. of Aeronautical Engineering
Nagoya University

ABSTRACT

Two turbulence models have been used to simulate a typical flow around NACA-0012 at zero angle of attack. Those turbulence models are the Cebeci-Smith Model (CSM) and the Baldwin-Lomax Model (BLM). Analysis of these models in terms of turbulent boundary layer has also been carried out in which the differences in the predicted turbulent characteristics are made clear. The computed result is compared with the experimental data obtained from the transonic tunnel at Nagoya University.

1. Introduction

The flow field surrounding the modern aircraft configurations is highly complex, dominated by three-dimensional effects and flow separation, and can be properly modeled only through the numerical simulation of the three-dimensional unsteady Navier-Stokes equations. However, since it is costly researchers often use the solution of two-dimensional codes in place of the three-dimensional solutions. To be useful, the two-dimensional codes should be provided with a suitable turbulence model to account for the real flow phenomena such as separation which is often encountered in transonic airfoil flow.

In the present paper is presented a typical result of calculation using a finite difference scheme of NACA-0012 airfoil at the transonic speed. Two classical turbulence models are used, i.e. the Cebeci-Smith model (CSM)[1] and the Baldwin-Lomax model (BLM)[2]. Those models are considered to be quite acceptable for a flow with a mild pressure gradient.[3]

The main differences in these two models are in the determination of the length scale. The CSM requires the boundary layer thickness to define the length scale of the outer eddy viscosity. However, this might pose a difficulty due to the existence of shock and non-uniformity of inviscid flow. The BLM uses the criteria of maximum vorticity function to define the length scale, thus avoiding the calculation of the edge of the boundary layer.

The CSM is not provided with any means to predict the transition location, while the BLM assumes that the onset of turbulence is defined by evaluating the ratio of maximum eddy viscosity to molecular viscosity. This greatly influences the prediction of aerodynamic characteristics.

* 名古屋大学

The objective of the present paper is to clarify the differences of the CSM and the BLM in the boundary layer flow with emphasis in the turbulent onset. For this seems to greatly influence the aerodynamic prediction. Section 3 presents a typical result of the calculation of transonic flow at M = 0.8 and Reynolds number Re = 10^6 as compared with the experiemental data obtained at the transonic tunnel of Nagoya University. The computed aerodynamic forces by using these two models will be also presented. Finally, the concluding remarks are described in section 4.

2. Comparison of Turbulence Models

2.1 Turbulence Models

In the two-layer model, the turbulent viscosity needs to be formulated for inner and outer layer, respectively. This criteria is based on the fact that the flow differs in the near wall region from that in the far field from the wall. In the near wall region, the presence of the wall gradually reduces the influence of the turbulent viscosity and eventually damps at the wall surface.[4] In this region the velocity can be expressed as a linear function of the dimensionless distance from the wall. Slightly far from the wall where the influence of the wall decreases the velocity can be depicted by the log law formulation. Far from the wall region, Coles has suggested that it has the velocity profile of the wake type.[5]

In the inner layer region, which consists of the viscous sublayer and the log law region, the CSM is modeled by the Prandtl-van Driest formulation[1]:

$$\varepsilon_i = \{kyD\}^2 \left|\frac{\partial u}{\partial y}\right| \tag{1}$$

where

$$D = 1 - exp\ (-y/A) \tag{2}$$

$$A = 26\frac{\nu}{u_\tau} \tag{3}$$

$$u_\tau = \sqrt{\frac{\tau_w}{\rho}} \tag{4}$$

where $\kappa = 0.4$ is the von Karman constant and τ_w is the wall shear stress.

In the outer layer, the CSM employs the Clauser's expression together with the Klebanoff intermittency factor γ_c:

$$\varepsilon_o = \alpha\delta^* U_\infty \gamma_c \tag{5}$$

where $\alpha = 0.0168$ for high Reynolds number flow. In the low Reynolds number flow region it is a function of Reynolds number. The Klebanoff intermittency factor is defined as:

$$\gamma_c = \{1 + 5.5\ (\frac{y}{\delta})^6\}^{-1} \tag{6}$$

The displacement thickness is used to define the length scale of the outer layer eddy viscosity. The determination of the length scale, which requires accurate calculation of boundary layer thickness, is difficult due to spurious oscillation of numerical solution.

To avoid these difficulties, the BLM applies the maximum vorticity function to define the length scale of the outer layer eddy viscosity. Thus, the outer eddy viscosity is expressed as follows:

$$\varepsilon_o = \alpha B_1 f_w \gamma_b \tag{7}$$

where B_1 = 1.6 is proposed. However, it was shown by Granville[6] and York and Knight[7] that B_1 is a function of the Coles wake factor.

$$f_w = \min\{y_{max} V_{max},\ B_{2ymax} U_{dif}^2 / V_{max}\} \tag{8}$$

where B_2 = 0.25 and V_{max} is the maximum value of the vorticity function:

$$V = y|\omega|D \tag{9}$$

y_{max} is the distance at which the function (9) gives the maximum value. The Klebanoff intermittency factor somewhat differs from that of eq. (6):

$$\gamma_c = \{1 + 5.5\,(\frac{B_3 y}{y_{max}})^6\}^{-1} \quad (10)$$

where $B_3 = 0.3$.

The BLM uses the Prandtl-van Driest formulation with a slight modification:

$$\varepsilon_i = \{kyD\}^2 |\omega| \quad (11)$$

where ω is the vorticity. Therefore, both models pose no significant differences in the inner layer.

The eddy viscosity of two-layer model is defined by

$$\varepsilon = \begin{cases} \varepsilon_i & \text{if } y \le y_c \\ \varepsilon_o & \text{if } y > y_c \end{cases} \quad (12)$$

where y_c is the smallest value where $\varepsilon_i = \varepsilon_o$.

The effect of transition from laminar to turbulent flow is defined by the ratio of the calculated eddy viscosity to the free stream molecular viscosity. The turbulence is initiated when the maximum ratio for a velocity profile exceeds a specified value.

$$\varepsilon = 0 \quad \text{if} \frac{\varepsilon_{max}}{\nu_\infty} < B_4 \quad (13)$$

where $B_4 = 14$. In the present calculation, the above criteria is used to determine the onset of turbulence.

2.2 Analysis of Turbulent Boundary Layer

The mean velocity profile of the turbulent boundary layer for mildly separated or non-separated flow with pressure gradient can be depicted with adequate accuracy by the two parameter Coles' wake function[6),(7)]:

$$\frac{U_\infty - u}{u_\tau} = \frac{\Pi}{k}\{2\text{–}2\sin^2(\frac{\pi}{2}\frac{y}{\delta})) - \ln(\frac{y}{\delta})\} \quad (14)$$

where Π is the Coles wake factor which varies with the Reynolds number in the low Reynolds flow region, $u_\tau = \sqrt{\tau_w/\rho}$ is the friction velocity, and τ_w is the wall shear stress. To evaluate the above-mentioned turbulence models, from eq. (14) one obtains

$$\left| y\frac{\partial u}{\partial y} \right| = \frac{u_\tau}{\kappa}\{2\pi\Pi\frac{y}{\delta}\sin(\frac{\pi}{2}\frac{y}{\delta})\cos(\frac{\pi}{2}\frac{y}{\delta}) + 1\} \quad (15)$$

The maximum property of $|y\partial u/\partial y|$ is located where

$$\frac{y_{max}}{\delta} = 0.646 \quad (16)$$

which suggests the proportionality of the length scale derived from the maximum vorticity function eq. (9) with the boundary layer thickness δ. This criteria 8) has enabled us to directly calculate the CSM. Stock and Haase used this criteria along with the adaptive grid to calculate the transonic flow around airfoil 8). Furthermore, they suggest that the increasing of the proportional factor by 25% will give a satisfactory result.

Accordingly, one may obtain from eq. (15) the following expression:

$$\left| y\frac{\partial u}{\partial y} \right|_{max} = \frac{u_\tau}{\kappa}(1.819\Pi + 1) \quad (17)$$

From the above expression, the relation between the displacement thickness and the friction velocity can be obtained as

$$\delta^* = \frac{u_\tau}{U_\infty}\frac{\delta}{\kappa}(\Pi + 1) \quad (18)$$

Then, equation (1) can be written in the dimensionless form

$$\tilde{\varepsilon}_{csm} \equiv \frac{\varepsilon}{\nu_\infty} = \alpha Re_{\delta^*} \quad (19)$$

Substituting eqs. (17) and (18) into eq. (8) leads to

$$\tilde{\varepsilon}_{blm} = \alpha Re_{\delta^*} C_1 \frac{(1.819\Pi + 1)}{\Pi + 1} \quad (20)$$

where $C_1 = 1.034$.

If the transition criteria assumed by Baldwin-Lomax is valid, then the transition location predicted by both models can be described as a function of Coles wake factor, which is presented

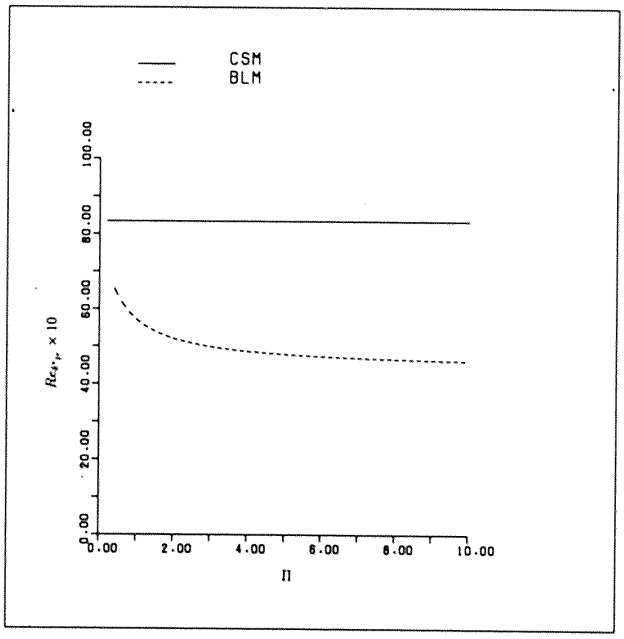

Fig. 1 Transition location

in Fig. 1. It is shown that in terms of Baldwin-Lomax transition criteria the CSM will predict the onset of turbulence more downstream than the BLM.

Moreover, the value of the maximum eddy viscosity by using the BLM is somewhat higher than the CSM. In no pressure gradient flow, this difference reaches as high value as 30%, which might mean the over-prediction of the boundary layer thickness.

3. Calculated Results

The numerical scheme used in the present study to solve the thin-layer Navier-Stokes equations for compressible flow is the same as described in ref. 9). The steady state is assumed to be reached when the relative error for every flow variable becomes less than 10^{-4}. Each case converged at about 850 steps. It required 110 seconds on Fujitsu FACOM VP200.

A 201 x 30 albegraically generated C grid is used, where 120 grid points are placed on the airfoil surface. The outer boundary is 10 chord lengths away from the body. To simulate the separation which is often encountered in the transonic airfoil the grid is refined up to the viscous sublayer. The first grid point away from the wall is in the order of 10^{-4}.

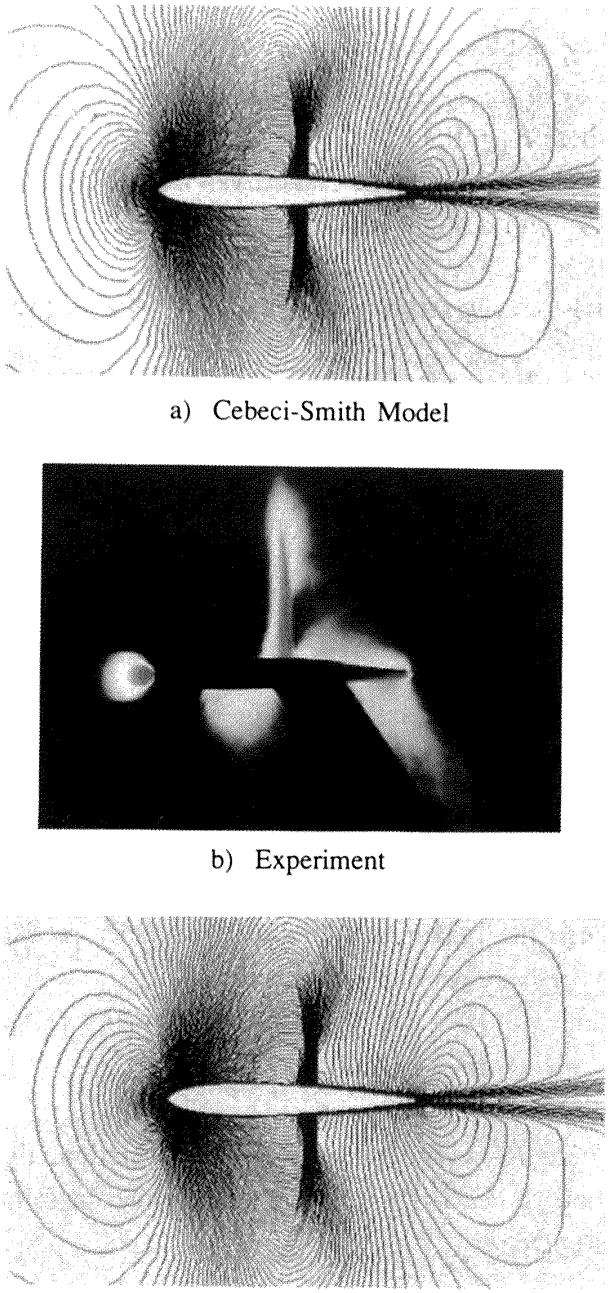

a) Cebeci-Smith Model

b) Experiment

c) Baldwin-Lomax Model

Fig. 2 Density contour and schlieren picture

Typical transonic flow solutions for NACA-0012 airfoil were computed for $Re = 10^6$ and $M_\infty = 0.8$. All computations were carried out up to the time when the mean flow travels by 5.3 chord length.

Figure 2 shows the isodensity line. Contours are made for $0.6 \leq \rho/\rho_\infty \leq 1.35$ in increment of 0.03. Schlieren picture which is known to represent the density gradient, obtained from the

experiment at the transonic tunnel is included for comparison. The agreement of the solution with the experiment is good, and the shock is well predicted.

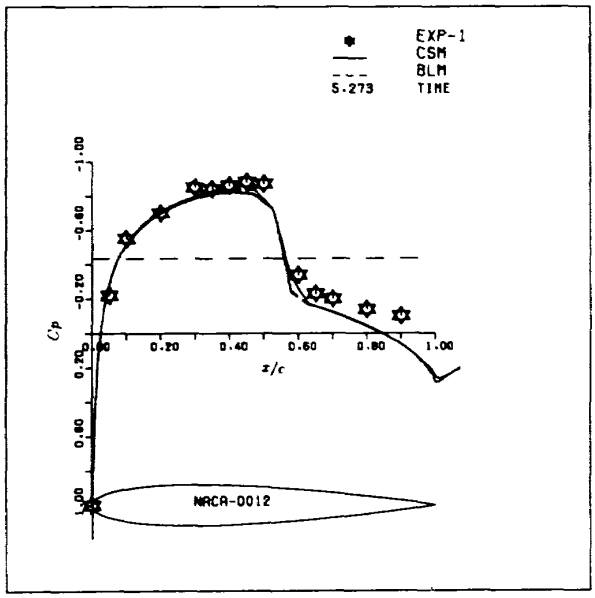

Fig. 3 Pressure distribution

Comparison of the computed surface pressure distribution with the experimental data is shown in Fig. 3. Upstream of the interaction, the agreement is good. The shock location is well captured, which has also been confirmed by the schlieren picture. A slight difference which can be noted here is the strength of the shock. The BLM's solution is rather weaker than the CSM. This might be associated with the fact that the eddy viscosity calculated by the BLM is higher than the CSM downstream of the shock. Both models cannot imitate the pressure plateau seen in the experiment which reveals the separation in the trailing edge region.

The turbulent eddy viscosity ε which is made non-dimensional by the free stream molecular viscosity ν_∞, is plotted in the x-direction at several stations in Fig. 4. The result reconfirms the above-mentioned bounday layer analysis that the

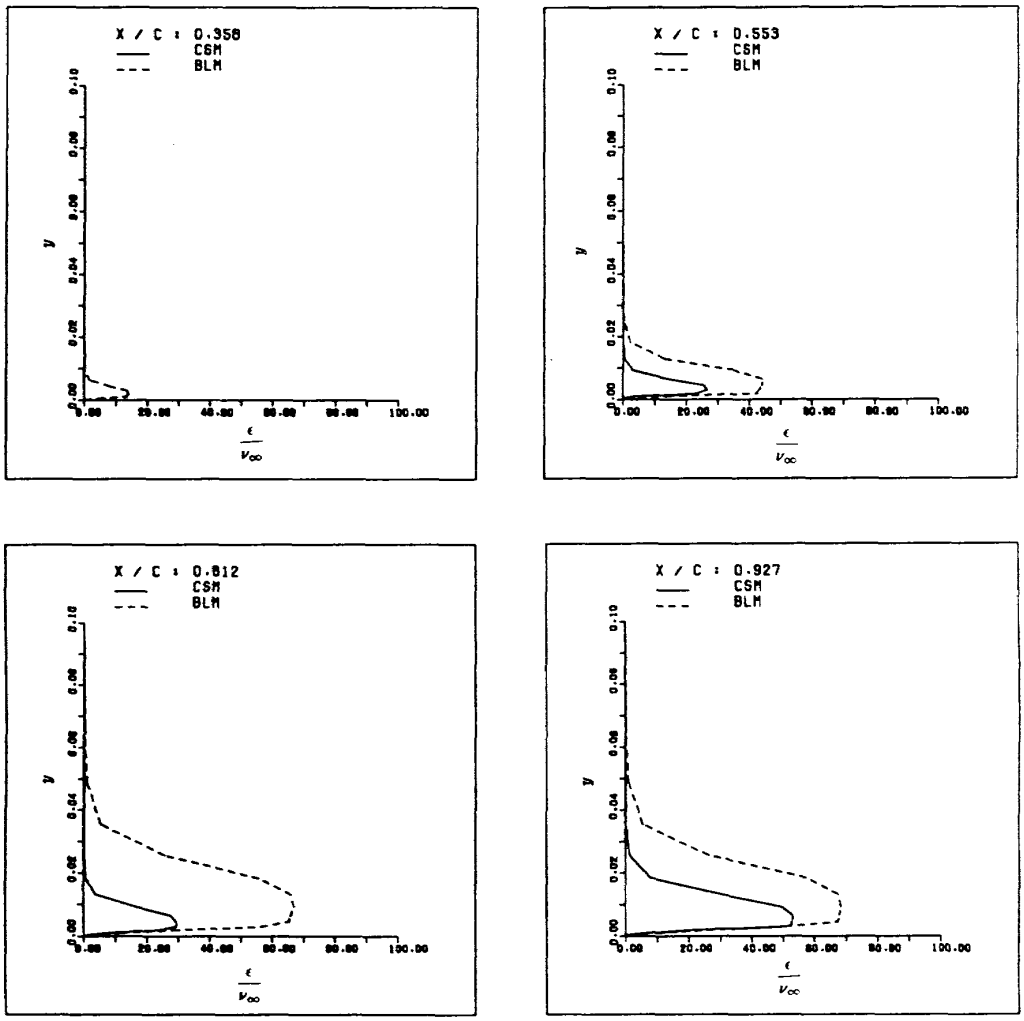

Fig. 4 Eddy viscosity profiles

maximum eddy viscosity calculated by the BLM is larger than that of the CSM.

The velocity distributions for both results are presented at several stations in Fig. 5. Both models predict similar velocity profiles, except in the shock region, where the inclined velocity profile can be seen for the CSM. Detailed inspection shows that in this region the CSM produces the negative velocity near the wall which indicates a reversed flow. This might be due to the reason that the CSM predicts with better computed pressure distribution, compared with the experiment in the redeveloping region downstream of the interaction.

The shear stress depends on both the velocity gradient and the eddy viscosity at the wall. The caclculated shear stresses from both turbulence models are plotted in Fig. 6 at several stations. It can be seen that the shear stresses for the BLM and the CSM are comparable.

The skin friction computed from both models is presented in Fig. 8. Again, upstream of the interaction, the skin friction is in good agreement. It is observed that the skin friction calculated by the BLM yields a sudden increase upstream of the shock, whereas the CSM's does not have such feature. This significant difference between two models might be related to the difference in predicted locations of transition, which has been ensured in the boundary layer analysis; the transition location of the BLM is more upstream than the CSM. This seems to be reasonable since in the accelerated flow region the eddy viscosity of the BLM is larger than that of the CSM, thus initiating the turbulent flow more upstream.

In attempt to make a comparison between the experiment and the calculation, the oil flow result is included. It can be observed that the "line" of

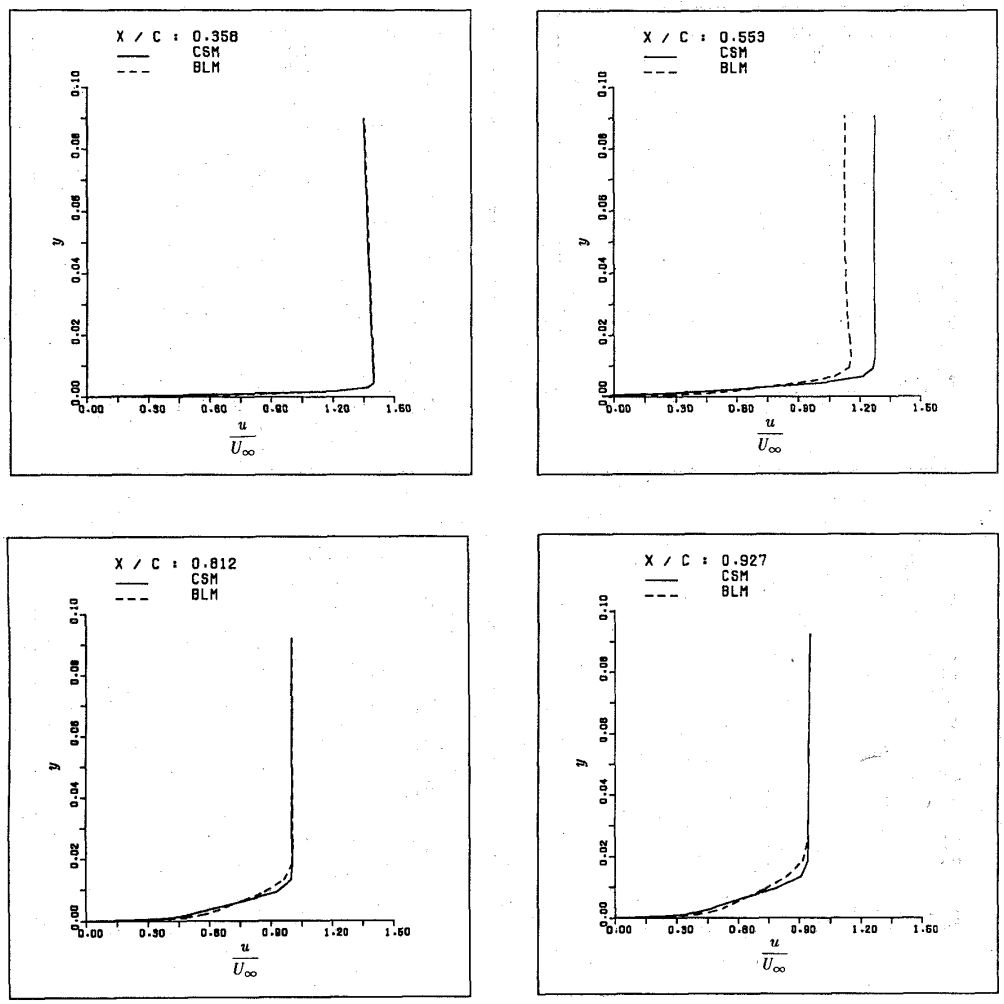

Fig. 5 Velocity profiles

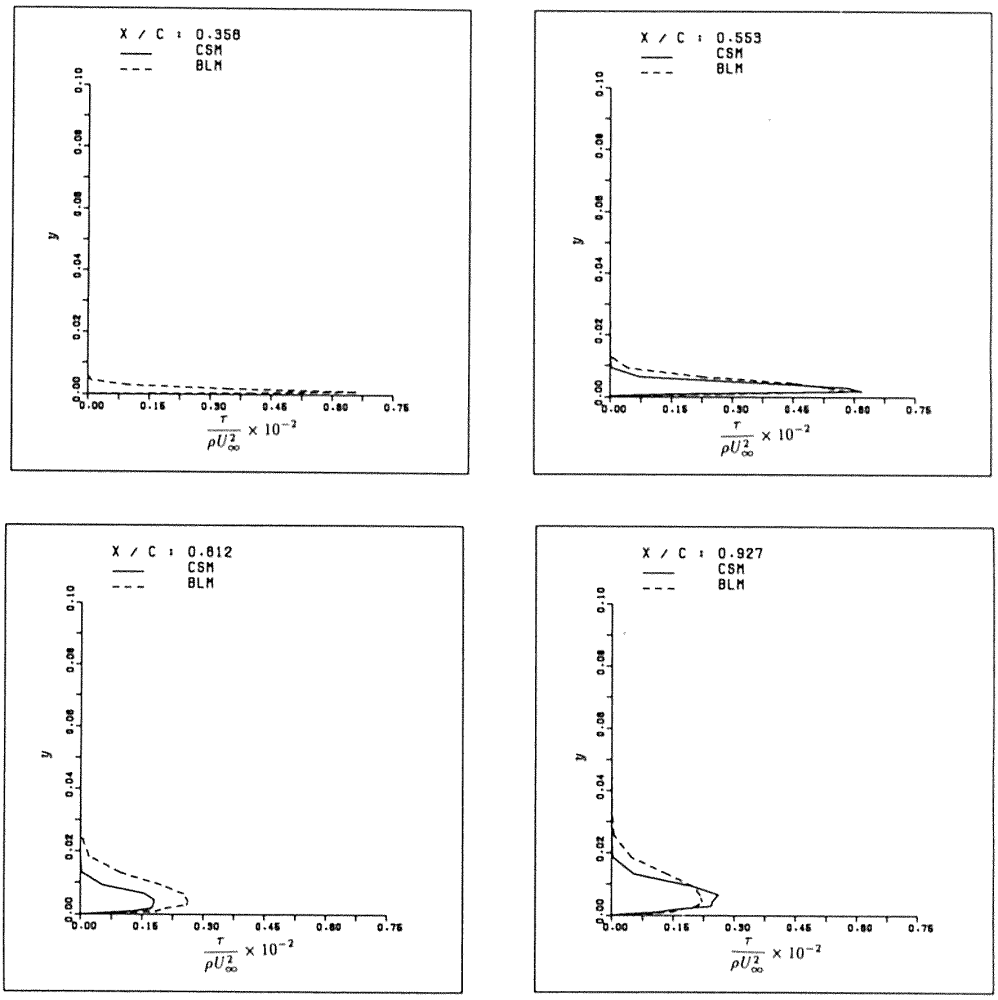

Fig. 6 Shear stress profiles

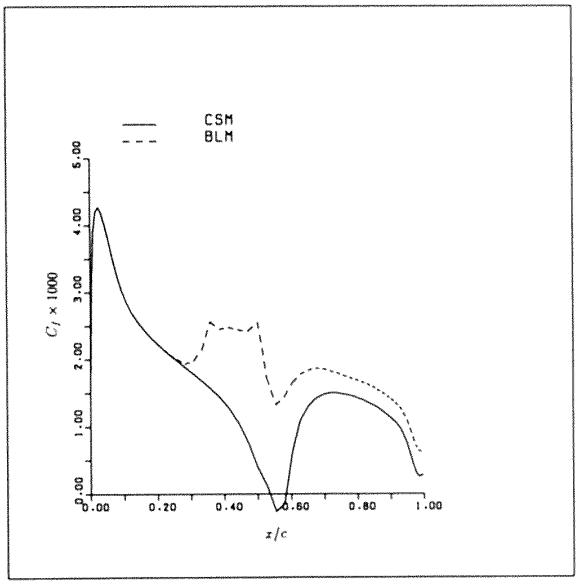

Fig. 7 Skin friction

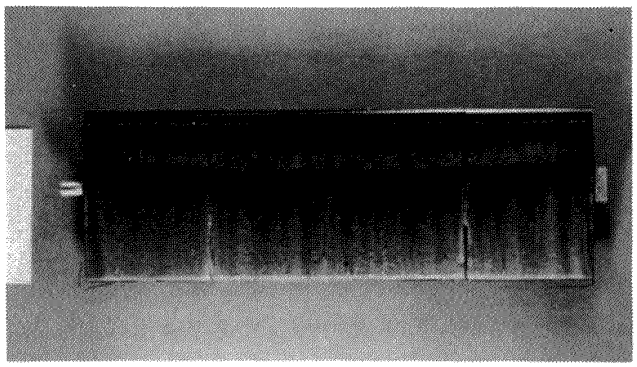

Fig. 8 Oil flow result as $M_\infty = 0.8$ and $\alpha = 0°$

transition is noticeable as the white line across the chord. It is located at approximately 30% of the chord, which agrees with the BLM prediction.

On the shock location, the CSM shows negative skin friction, which means that the model can predict a separation. Comparing with the experimental result, which is characterized by the plateau pressure distribution. This which shows the plateau pressure distribution on this location. This might reconfirm the Stock-Haase method that to avoid the bounded eddy viscosity in the separation

region, the displacement thickness might be calculated better if we started from the distance where the stream velocity is zero instead of on the wall.[8]

The present study will be concluded by showing the computed drag. Here the drag is computed by using the widely known Squire-Young formula, which is defined as [1]:

$$C_D = 2\left(\frac{\theta}{c}\right)\left(\frac{U_{te}}{U_\infty}\right)^{\left(\frac{H_{te}+5}{2}\right)} \qquad (21)$$

where H is the shape factor ($H = \delta^*/\theta$). δ^* and θ are the displacement thickness and the momentum thickness, respectively. Here, the subscript te denotes the trailing edge location and c is the chord length. The predicted drag coefficients of NACA-0012 at $Re = 10^6$, $M = 0.8$ and zero angle of attack are presented for both turbulence models in Table 1.

Table 1. Predicted Drag Coefficients of NACA-0012

Turbulence Model	Drag Coefficient
CSM	0.003683
BLM	0.005778
Exp. [10]*	0.005683

*) $Re = 3 \times 10^6$

The large difference in the predicted drag coefficient may be due to the difference in predicted transition location. Even if the classical Michele[1] expression is employed to predict the transition location which is based on the displacement thickness Reynolds number, the same result will be obtained, since the main cause is due to the difference in the predicted eddy viscosity, which may in turn cause the difference in the boundary layer thickness.

4. Concluding Remarks

It has been shown in this study that from the turbulence boundary layer study, the BLM predicts larger eddy viscosity than the CSM mainly in the outer region. This may cause the difference in the boundary layer thickness.

The simple prediction of transition location based on the ratio of the maximum eddy viscosity to the molecular viscosity in the velocity profile seems to be adequate for the BLM but is somewhat rather higher for the CSM. Thus, it leads to the significant differences in aerodynamic force prediction.

References

1) Cebeci, S. and Smith, A.M.O.: *Analysis of Turbulent Boundary Layers*, Academic Press, 1974.
2) Baldwin, B. and Lomax, H.: *Thin Layer Approximation and Algebraic Model for Separated Turbulent Flows*, AIAA Paper 78-257, 1978.
3) Lakshminarayana, B.: *Turbulence Modeling for Complex Shear Flows*, AIAA J., Vol. 24, 1986, pp. 1990-1917.
4) Van Driest, E.R.: *On Turbulent Flow Near a Wall*, J. of Aero. Sci., 1956, pp. 1007-1011.
5) Coles, D.: *The Law of the Wake in Turbulent Boundary Layer*, JFM, Vol. 1, 1956, pp. 191-226.
6) Granville, P.S.: *Baldwin-Lomax Factors for Turbulent Bounday Layers in Pressure Gradients*, AIAA J., Vol. 25, 1987, pp. 1624-1627.
7) York, B. and Knight, D.: *Calculation of Two-Dimensional Turbulent Boundary Layers using the Baldwin-Lomax Model*, AIAA J., Vol. 23, 1985, pp. 1849-1850.
8) Stock, H.W. and Haase, W.: *Determination of Length Scales in Algebraic Turbulence Models for Navier-Stokes Methods*, AIAA J., 1989, pp. 5-14.
9) Yee, H.D. and Harten, A.: *Implicit TVD Scheme for Hyperbolic Conservation Laws in Curvilinear Coordinate*, AIAA Paper 85-1513, 1985.
10) Abbott, I.H. and Doenhoff, A.V.: *Theory of Wing Sections*, Dover, 1959.